ECOLOGY LETTERS

Ecology Letters, (2013) **16**: 56–63 doi: 10.1111/ele.12012

LETTER

Functional traits explain phytoplankton community structure and seasonal dynamics in a marine ecosystem

Kyle F. Edwards,[1]* Elena Litchman [1,2] and Christopher A. Klausmeier [1,3]

Abstract

A fundamental yet elusive goal of ecology is to predict the structure of communities from the environmental conditions they experience. Trait-based approaches to terrestrial plant communities have shown that functional traits can help reveal the mechanisms underlying community assembly, but such approaches have not been tested on the microbes that dominate ecosystem processes in the ocean. Here, we test whether functional traits can explain community responses to seasonal environmental fluctuation, using a time series of the phytoplankton of the English Channel. We show that interspecific variation in response to major limiting resources, light and nitrate, can be well-predicted by lab-measured traits characterising light utilisation, nitrate utilisation and maximum growth rate. As these relationships were predicted *a priori*, using independently measured traits, our results show that functional traits provide a strong mechanistic foundation for understanding the structure and dynamics of ecological communities.

Keywords

Marine, microbial, multilevel/hierarchical models., trait-based ecology.

Ecology Letters (2013) **16**: 56–63

INTRODUCTION

One of the longstanding challenges facing ecologists is to predict the structure and dynamics of communities from the environmental conditions they experience. Although it is straightforward to document how species composition changes over time or along spatial gradients, it is much more difficult to identify the mechanisms that determine the rise and fall of abundances. In fact, the sheer number of abiotic and biotic factors that affect populations, combined with the intricacy of networks of interacting species, has at times made ecological communities seem intractably complex (Lawton 1999). However, it has been argued that a renewed focus on species' functional traits may lead to improved mechanistic linkages between environmental drivers and the composition of communities (McGill *et al.* 2006; Litchman & Klausmeier 2008). This approach is supported largely by a growing body of work on terrestrial plants, showing that the community-wide distributions of traits change across environmental gradients. For example, mean specific leaf area increases with soil water content in coastal Californian plant communities (Cornwell & Ackerly 2009), and mean wood density of trees increases with mean annual temperature and precipitation in eastern North America (Swenson & Weiser 2010). Patterns such as these link the performance of a species in a particular environment to that species' phenotype, providing insights into the mechanisms by which abiotic conditions combine with species interactions to assemble communities across environmental gradients. Building from these approaches, it may ultimately be possible to predict community trait structure from first principles of physiology and morphology.

Although some progress has been made on the trait-based community ecology of terrestrial plants, a tight linkage between traits and community structure has not been established for the phytoplankton and other microbes that dominate ecosystem processes in the ocean. Field and lab studies of marine and freshwater systems have shown that numerous factors can control phytoplankton community composition, including nitrogen, phosphorus, silica, iron, light, temperature and grazers (Tilman *et al.* 1982; Berquist *et al.* 1985; Landry *et al.* 2000; Johnson *et al.* 2006; Stomp *et al.* 2007). Ecophysiological lab studies have documented how these factors affect cellular processes and population growth, and how responses to these factors differ between species (e.g. Eppley *et al.* 1969; Briand & Guillard 1981; Moore *et al.* 1995). Population dynamic models have been parameterised using ecophysiological traits, and these models have been shown to predict the outcome of competition in lab cultures (Tilman 1977; Grover 1991; Passarge *et al.* 2006). In some cases, the relative abundance across environmental gradients of a few dominant species or functional groups has been predicted from such models (Tilman 1977; Smith 1983; Huisman *et al.* 2004; Stomp *et al.* 2007; Elliott *et al.* 2010). Thus, the accumulation of work on phytoplankton community structure and functional traits suggests that these traits may be effective predictors of how environmental conditions determine the differential success of species. In addition, a better understanding of the processes that structure phytoplankton communities is essential, because they account for roughly half of global primary production and affect the biogeochemical cycling of many elements (Falkowski *et al.* 2004), and because phytoplankton community composition can impact global climate (Falkowski *et al.* 1998), the trophic dynamics of aquatic ecosystems (Sterner & Elser 2002) and water quality (Anderson *et al.* 1998).

The approach we take here builds upon the use of functional groups. Oceanographers and limnologists have long divided

[1]*Kellogg Biological Station, Michigan State University, Hickory Corners, MI, 49060, USA*
[2]*Department of Zoology, Michigan State University, East Lansing, MI, 48824, USA*
[3]*Department of Plant Biology, Michigan State University, East Lansing, MI, 48824, USA*
**Correspondence: E-mail: edwar466@msu.edu*

phytoplankton into groups based on taxonomy or morphology, and documented how these groups shift in importance across environmental conditions (Margalef 1978). As representatives of these groups have been studied in the lab, shifts in the relative abundance of functional groups can be putatively associated with shifts in community trait composition (e.g. Boyd *et al.* 2010; Bouman *et al.* 2011; Kruk *et al.* 2011). However, trait compilations show that key functional traits exhibit high variance within functional groups, and large overlap between functional groups (e.g. Schwaderer *et al.* 2011; Edwards *et al.* 2012). Therefore, a higher resolution approach, utilising species- or strain-specific trait data, will be necessary to test whether the success of phytoplankton in communities can be directly linked to functional traits.

Here, we test whether a suite of functional traits can explain how the phytoplankton community of a temperate marine ecosystem, the Western English Channel sampled at station L4, varies in response to seasonal fluctuation in light and nutrients. Seasonal fluctuation in this system follows the paradigmatic pattern for coastal temperate waters, where the dominating factor is the depth to which phytoplankton are mixed by turbulence (Longhurst 2007; Smyth *et al.* 2010; Widdicombe *et al.* 2010; Fig. 1): the water column is well-mixed during the autumn and winter due to low temperature and high wind, while stratification during the spring and summer leads to a surface mixed layer; as irradiance in the shoaling mixed layer increases during the spring, a bloom occurs; algal growth reduces nitrate to very low concentrations that are thought to limit growth during the summer; a second algal bloom occurs during the fall as stratification weakens and nutrient-rich water is entrained into the mixed layer; and algal abundance decreases to low levels during the winter, when low irradiance in the well-mixed water column is thought to limit growth. Therefore, aggregate production is likely limited by light during the winter and nitrogen during the summer, with intervening bloom periods when resource limitation is alleviated (Fig. 1). At the same time, community composition shifts over this annual cycle (Widdicombe *et al.* 2010), implying that species respond differentially to varying abiotic conditions.

We can quantify differential responses to environmental factors as differences between species in slopes of abundance vs. those factors. Initial inspection of a long-term time series indicated that most species tend to be more abundant when nitrate is scarce or when light (PAR, photosynthetically active radiation) is high, because these conditions occur from spring to fall, when total biomass is greater; however, there is interspecific variation in the steepness of the slope of these relationships (Figs S3–S4). Likewise, we can quantify overall resource availability, that is, non-limiting conditions, as the product nitrate*PAR; in general, abundance increases as nitrate*PAR increases, with interspecific variation in the strength of this response (Fig. S5). The analysis we present below is designed to test whether commonly measured functional traits can predict these differences between species in the slope of response to environmental factors. Because of the dominant roles of light and nitrate in this system, we use traits related to competitive ability for nitrate, tolerance of low light and growth rate in the absence of resource limitation. We make the following predictions for how these traits affect differential responses (Fig. 2): species that are better competitors for nitrate should have a relative advantage when nitrate is scarce, and as a result will have a more negative slope of abundance vs. nitrate; species with greater tolerance of low light should have a relative advantage when light is low, and as a result will have a less positive or more negative slope of abundance vs. PAR; and species with higher maximum growth rate should have a relative advantage when nitrate*PAR is high, and as a result will have a more positive slope of abundance vs. nitrate*PAR.

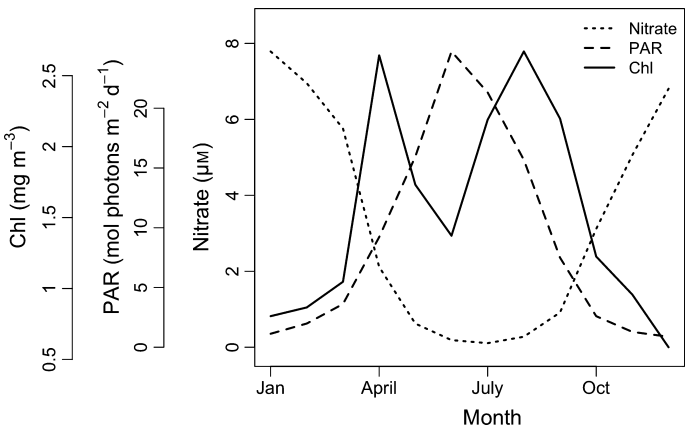

Figure 1 Intraannual variation in surface nitrate, mean mixed-layer photosynthetically active radiation and surface chlorophyll at the L4 station. Values for each month are monthly averages over all years in the analysis.

We note that our depiction of differential responses in Fig. 2 is tailored to phytoplankton in the Western English Channel. As conditions from spring to fall are generally more favourable for phytoplankton (Fig. 1), most species are more abundant at times when nitrate is low and PAR is high. Our predictions concern the variation between species in these overall trends, but we expect that the same general predictions should hold under other conditions. For example, in some systems there may be an overall positive correlation between nitrate concentration and abundance, for example, if variation in nitrate concentration is driven by variation in nitrate supply rate. In such a system, we would again predict that better nitrate competitors should have a more negative (less positive) slope of abundance vs. nitrate, because they would have a relative advantage when nitrate is scarce.

METHODS

The L4 time series

We take advantage of the excellent oceanographic time series produced and maintained by the Western Channel Observatory (http://www.westernchannelobservatory.org.uk). The L4 station is located at 50°15.00′ N, 4°13.02′ W, 10 km south of Plymouth breakwater, with a nominal depth of 51 m (Harris 2010). Phytoplankton at 10 m depth have been sampled and counted on a weekly or biweekly basis since 1992 (for more details on phytoplankton methods, see Widdicombe *et al.* 2010). Other data collected at L4 and used in this study include surface nutrients, chlorophyll and depth-profiled temperature (collection methods for these data are described in Smyth *et al.* 2010). Estimated daily integrated incident photosynthetically active radiation (PAR), calculated from a spectral model and cloud cover data, was kindly provided by T.J. Smyth (Smyth *et al.* 2010). As these different variables were not always measured synchronously, we averaged each variable by month, and used these monthly averages in all subsequent analyses. The resulting time series includes data from Sep. 2002 to Dec. 2009. Monthly averages are reasonable for this analysis, because the

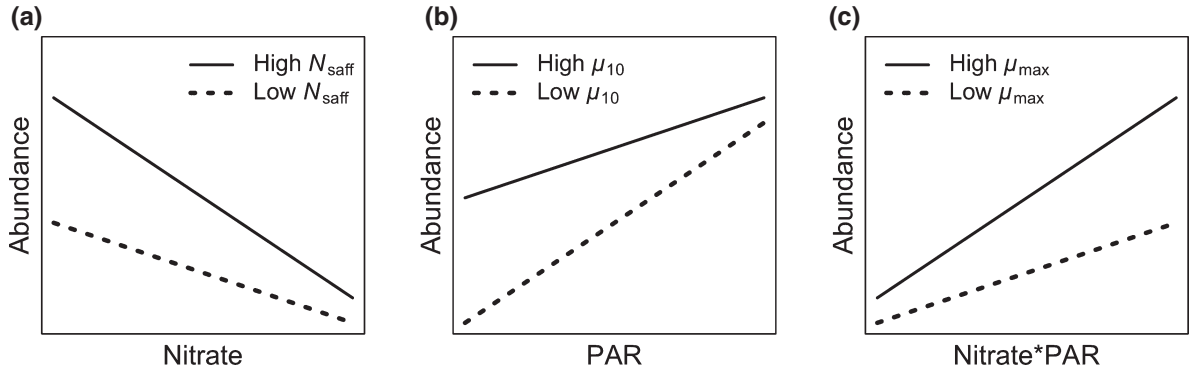

Figure 2 Predicted effects of the three functional traits on species' responses to environmental variation. The relative mean height of the lines is arbitrary, because the predictions concern the relative steepness of the slopes. (a) Species with higher competitive ability for nitrate (higher N_{saff}) should increase more steeply as ambient nitrate concentration decreases, due to a competitive advantage when nitrate is limiting. (b) Species with greater tolerance of low light (higher μ_{10}) should decline less steeply as photosynthetically active radiation (PAR) declines, due to a greater ability to tolerate low PAR. (c) Species with greater maximum growth rate (higher μ_{max}) should increase more steeply as nitrate*PAR increases, due to faster growth under non-limiting conditions.

dominant source of environmental variation is between different seasons (Fig. S1). We also performed the same analysis using biweekly averages, and found the same functional trait effects.

To quantify variation in irradiance available to phytoplankton in the mixed layer, we estimated mean PAR in the mixed layer. The depth of the mixed layer (MLD) was estimated using a threshold method (Thomson & Fine 2003), in which the MLD was the depth at which the temperature was at least 0.2 °C less than the temperature at 2 m (the shallowest depth measured). Attenuation of incident PAR through the mixed layer was estimated using an attenuation coefficient at 440 nm for seawater of 0.015 m^{-1} (based on Kirk 1994); for chlorophyll of 0.025 mg^{-1} m^2 (based on Kirk 1994); and for dissolved organic matter of 0.075 m^{-1}, based on typical values at L4 (http://www.westernchannelobservatory.org.uk/l4_cdom.php). Our results are robust to changes in the calculation of mean mixed-layer PAR, and if we use only incident PAR to represent light availability, we find the same functional trait effects as reported in the Results. Time series of nitrate and PAR are shown in Fig. S1 (Supporting Information).

Measurement of phytoplankton ecophysiological traits requires labour-intensive laboratory culture methods. Thus, the trait data we use are compiled from many published studies and cover only a subset of the species recorded at L4. There are eleven species for which we have trait data for all of the traits described below: the diatoms *Coscinodiscus wailesii*, *Ditylum brightwellii*, *Eucampia zodiacus*, *Nitzschia closterium*, *Pseudo-nitzschia pungens*, *Skeletonema costatum* and *Asterionellopsis glacialis*; the coccolithophore *Emiliania huxleyi*; and the dinoflagellates *Alexandrium tamarense*, *Prorocentrum micans* and *Gymnodinium catenatum*. These species range from common to rare at L4 (Fig. S2), and represent the dominant taxonomic groups of larger phytoplankton in this system. Smaller taxa such as cyanobacteria or prasinophytes are not represented, but the species we focus on have a broad range of trait values (Fig. 3), and thus, it is reasonable to consider them as a sample from the full range of trait variation. Sources for functional traits are listed in Table S1.

Functional traits

Our analysis uses five functional traits, three related to nitrate utilisation, one related to light utilisation and finally maximum growth rate. We characterise nitrate utilisation with scaled uptake affinity for nitrate (N_{saff}), which is a composite of three functional traits:

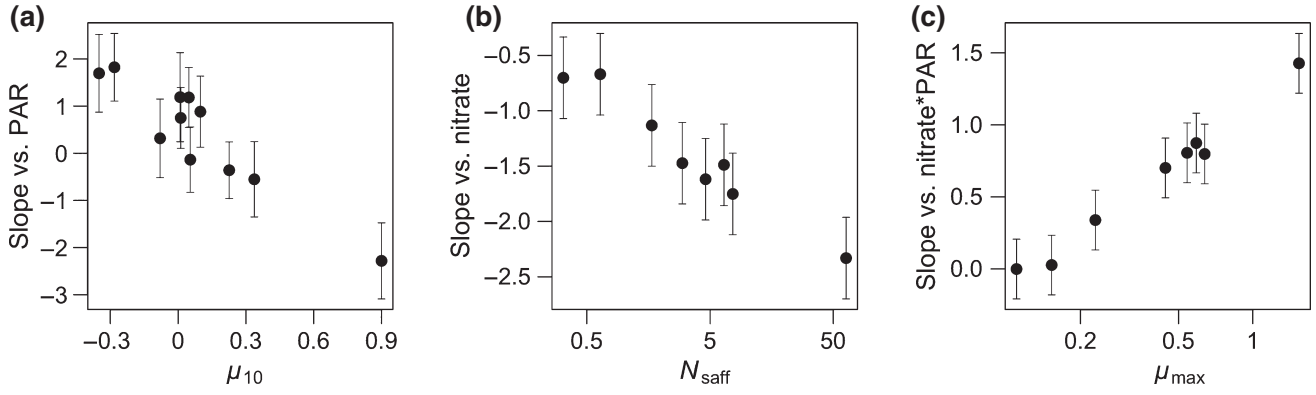

Figure 3 Model-fitted slopes and their relationship to the three functional traits. Points are posterior means, error bars are ± 1 posterior standard deviation. (a) Slope of response to PAR ($b^i_{PAR} + \gamma_{PAR*\mu10}\mu^i_{10}$) in the occurrence model vs. μ_{10}. The effect of μ_{max} on response to PAR ($\gamma_{PAR*\mu max}\mu^i_{max}$) is removed, to visualise the effect of μ_{10}. (b) Slope of response to nitrate ($b^i_{nit} + \gamma_{nit*N}N^i_{saff}$) in the abundance model vs. N_{saff} (log scale). The effect of μ_{max} on response to nitrate ($\gamma_{nit*\mu max}\mu^i_{max}$) is removed, to visualise the effect of N_{saff}. (c) Slope of response to nitrate*PAR ($b^i_{n*P}+\gamma_{n*P*\mu max}\mu^i_{max}$) in the abundance model vs. μ_{max} (log scale).

maximum cell-specific nitrate uptake rate (V_{max}), the half-saturation constant for nitrate uptake (K) and the minimum nitrogen quota (Q_{min}). V_{max} and K are the parameters of the Michaelis–Menten curve typically fitted to measurements of uptake rate as a function of nutrient concentration in the medium. Uptake affinity ($\frac{V_{max}}{K}$) is the slope of the Michaelis–Menten curve at the origin, which quantifies the cell-specific clearance rate for a nutrient, as nutrient concentration nears zero (Healey 1980). Q_{min} is typically estimated when fitting the Droop model of phytoplankton growth (Droop 1973), which relates growth rate to internal nutrient content such that $\mu(Q) = \mu_\infty\left(1 - \frac{Q_{min}}{Q}\right)$, where $\mu(Q)$ is specific growth rate as a function of Q, Q is cellular internal nutrient concentration or quota, Q_{min} is the minimum quota at which growth ceases, and μ_∞ is asymptotic growth rate at infinite quota. Therefore, scaled uptake affinity ($\frac{V_{max}}{KQ_{min}} = N_{saff}$) combines these three traits to scale uptake ability (affinity) by the amount of nitrogen required for growth. Furthermore, in a model where Michaelis–Menten uptake is coupled to the Droop growth equation, N_{saff} predicts the winner of nutrient competition at equilibrium, in the limit of zero mortality (Edwards *et al.* 2011). In a compilation of chemostat studies, we found that scaled uptake affinity is a good predictor of the winner in competition at equilibrium, even at relatively high mortality rates (=dilution rates) (Edwards *et al.* 2012). We therefore consider N_{saff} to be a good proxy of competitive ability for nitrate under limiting conditions. We note that in a prior study (Edwards *et al.* 2011), N_{saff} was referred to as 'competitive ability for nitrate', or C^N; we now prefer N_{saff}, which better highlights the relationship between this trait and uptake affinity. We compiled estimates of V_{max}, K and Q_{min} from published studies in which cultures were maintained at or near 20 °C and light was not severely limiting (Table S1).

A species' light utilisation is often characterised in the lab by measuring growth rate as a function of irradiance. This relationship is typically well-fit by the following curve:

$$\mu(I) = \frac{p_{max} I}{\frac{p_{max}}{\alpha I_{opt}^2} I^2 + (1 - 2\frac{p_{max}}{\alpha I_{opt}})I + \frac{p_{max}}{\alpha}} - r, \quad (1)$$

where $\mu(I)$ is specific growth rate as a function of irradiance I, p_{max} is maximum production rate, α is the slope of the curve when $I = 0$, I_{opt} is the irradiance at which p_{max} is achieved and r is the respiration/loss rate (Eilers & Peeters 1988). This curve is unimodal with a peak at I_{opt}, and as photoinhibition approaches zero ($I_{opt} \to \infty$), the curve becomes a hyperbola with an asymptote at ($p_{max} - r$). In our analysis, we use this curve to calculate predicted growth rate at 10 μmol photons m^{-2} s^{-1} ($\mu(10)$, hereafter denoted μ_{10}). Growth rate at this irradiance should indicate the ability of a species to tolerate the low mean mixed-layer PAR typical of the Western English Channel during winter months, which reaches a December minimum of ~10 μmol photons m^{-2} s^{-1} (Fig. 1). We compiled data on growth vs. irradiance for each species from the literature, using studies in which cultures were maintained at or near 20 °C and nutrients were not severely limiting. For all cases in which original data was plotted, we extracted the data with ImageJ (Rasband 2011) and fit the curve (1) to estimate μ_{10}.

To quantify maximum growth rate, we used studies in which growth rate was measured as a function of temperature, under non-limiting resource conditions. This relationship can be characterised by the following curve:

$$\mu(T) = ae^{bT}\left(1 - \left(\frac{T - z}{w}\right)^2\right),$$

where $\mu(T)$ is growth rate as a function of temperature, and a, b, z and w determined the height, shape and location of a unimodal curve (Norberg 2004). We used this curve to calculate maximum growth rate (μ_{max}) for each species at a variety of temperatures. In our analysis, we used maximum growth rate at 12.5 °C, as that temperature gave the maximum explanatory power for predicting interspecific variation in response to nitrate*PAR. However, the results were very similar using growth at any temperature from 10 to 20 °C. The choice of 12.5 °C is biologically sensible, because temperature typically ranges from 10 to 13 °C during the spring bloom.

Statistical methods

As described in the Introduction, we expect the community to be structured by light limitation, nitrogen limitation and bloom periods when neither of these factors is strongly limiting. We hypothesise that μ_{10}, N_{saff} and μ_{max} will predict the relative performance of species under these different conditions. To test this hypothesis, we use statistical models in which species are allowed to vary in the slope of their response to PAR, nitrate and nitrate*PAR, and terms are included to test whether the functional traits predict interspecific variation in the relevant slopes (Fig. 2). Although we do not have relevant trait data for the full phytoplankton community of the English Channel, this approach addresses community-level trait structure because the differential responses of the component species result in shifting relative abundances (Fig. 2).

We use multilevel models (also known as mixed or hierarchical models) to test these predictions (Gelman & Hill 2006). Multilevel models are useful for a variety of ecological applications (Clark 2007) and have been proposed as a framework for trait-based analysis of community data (Webb *et al.* 2010). A key advantage of multilevel models is that multiple sources of variation can be accounted for in a single framework; in the current analysis, variation in abundance is partitioned into variation between species in response to environmental factors, variation between species not explained by environmental factors and variation not explained by species identity or environmental factors.

Abundances are recorded as densities (cells mL^{-1}), which results in a distribution for the data that is semi-continuous (continuous on the positive reals with positive mass at zero), with a large proportion of zeros for some species due to naturally large fluctuation in abundances and non-detection of rare species (Fig. S6). To account for this distribution, we used a two-stage conditional approach (Cunningham & Lindenmayer 2005), in which presence/absence was modelled as a binary response based on the predictors described below, and log abundance (biovolume L^{-1}), conditional on presence, was modelled as a function of the same predictors. We refer to these as the occurrence and abundance models respectively. Nitrate was quarter-root transformed, and PAR, N_{saff} and μ_{max} were log-transformed, to linearise relationships with the

response variables and ensure that rare large values of the predictors were not disproportionately influential. All predictors were then standardised by centring around their mean and division by their standard deviation, to aid model convergence and interpretation. To quantify a lack of limitation by nitrate or light, we created a new variable nitrate*PAR = $\left(\frac{nitrate-Min(nitrate)}{Max(nitrate)-Min(nitrate)}\right) * \left(\frac{PAR-Min(PAR)}{Max(PAR)-Min(PAR)}\right)$, where *nitrate* and *PAR* refer to the standardised versions of these predictors. Therefore, nitrate*PAR has a minimum of 0 where either factor is at its minimum value in the data set, and a maximum of 1 when both factors are at their maximum value.

The occurrence model can be written as

$$\text{logit}(\hat{p}_t^i) = \beta_0^i + \beta_{nit}^i nit_t + \beta_{PAR}^i PAR_t + \beta_{n*P}^i nitPAR_t + \rho Lag_t^i, \quad (2)$$

where logit() is the logit link function, $\hat{p}_t^i$ is the expected probability of presence for species i at time t, β_0^i is the species-specific intercept for species i, nit_t is nitrate concentration at time t, β_{nit}^i is the slope of species i against nitrate, PAR_t is mean mixed-layer PAR at time t, β_{PAR}^i is the slope of species i against PAR, $nitPAR_t$ is nitrate*PAR at time t, β_{n*P}^i is the slope of species i against nitrate*PAR, Lag_t^i is occurrence (0 or 1) of species i at time $t-1$ and ρ is the effect of lagged occurrence on occurrence at time t. Lagged occurrence is included in the model to account for temporal autocorrelation in occurrence not accounted for by the other predictors (Fig. S7); very similar results were found when using an autocorrelated random effect, and we use lagged occurrence here because it is computationally simpler.

Each of the β terms in eqn 2 is modelled as a function of the focal traits, while allowing for random interspecific variation not explained by these traits:

$$\begin{aligned}
\beta_0^i &= b_0^i + \gamma_N N_{\text{saff}}^i + \gamma_{\mu 10}\mu_{10}^i + \gamma_{\mu max}\mu_{\max}^i \\
\beta_{nit}^i &= b_{nit}^i + \gamma_{nit*N} N_{\text{saff}}^i + \gamma_{nit*\mu max}\mu_{\max}^i \\
\beta_{PAR}^i &= b_{PAR}^i + \gamma_{PAR*\mu 10}\mu_{10}^i + \gamma_{PAR*\mu max}\mu_{\max}^i \\
\beta_{n*P}^i &= b_{n*P}^i + \gamma_{n*P*\mu max}\mu_{\max}^i
\end{aligned} . \quad (3)$$

b_0^i, b_{nit}^i, b_{PAR}^i, and b_{n*P}^i are random effects for species i, distributed normally with respective means $\overline{b_0}$, $\overline{b_{nit}}$, $\overline{b_{PAR}}$, $\overline{b_{n*P}}$, and respective variances σ_0, σ_{nit}, σ_{PAR} and σ_{n*P}. These effects estimate unexplained interspecific variation in the intercept, slope vs. nitrate, slope vs. PAR and slope vs. nitrate*PAR respectively. γ_N, $\gamma_{\mu 10}$ and $\gamma_{\mu max}$ are, respectively, the effects of N_{saff}, μ_{10} and $\mu_{\max}$ when the environmental predictors are all zero (i.e. at their median values); γ_{nit*N} is the effect of N_{saff} on a species' slope vs. nitrate; $\gamma_{nit*\mu max}$ is the effect of $\mu_{\max}$ on a species' slope vs. nitrate; $\gamma_{PAR*\mu 10}$ is the effect of μ_{10} on a species' slope vs. PAR; $\gamma_{PAR*\mu max}$ is the effect of $\mu_{\max}$ on a species' slope vs. PAR; and $\gamma_{n*P*\mu max}$ is the effect of $\mu_{\max}$ on a species' slope vs. nitrate*PAR. Our *a priori* predictions concern these interactions between traits and environmental predictors: we predict that γ_{nit*N} and $\gamma_{PAR*\mu 10}$ should be negative, because species with higher trait values should have more negative or less positive slopes vs. nitrate and light, while $\gamma_{n*P*\mu max}$ should be positive, because species with higher trait values should have more positive slopes vs. nitrate*PAR (Fig. 2). The lower order effects $\gamma_{nit*\mu max}$ and $\gamma_{PAR*\mu max}$ are included to properly test for the higher order interactive effect of $\gamma_{n*P*\mu max}$.

The model for abundance conditional on presence is similar to eqn 2:

$$\log(V_t^i) = \beta_0^i + \beta_{nit}^i nit_t + \beta_{PAR}^i PAR_t + \beta_{n*P}^i nitPAR_t + \varepsilon_t^i, \quad (4)$$

where $\log(V_t^i)$ is log biovolume of species i at time t; ε_t^i is residual log biovolume, modelled to account for residual autocorrelation such that $\varepsilon_t^i = \rho^{t-\tau}\varepsilon_\tau^i + \nu_t^i$, where τ is the time of the most recent observed abundance for species i, and ν_t^i is normally distributed with mean zero and variance σ_ν (Fig. S8). The β terms in eqn 4 are also modelled according to eqn 3. For notational convenience, we use the same notation for the parameters of the occurrence and abundance models, although these models are fit separately. When parameters are reported in the Results, we state which model is being referred to. The species *Alexandrium tamarense, Gymnodinium catenatum* and *Asterionellopsis glacialis* were excluded from the abundance model, because they occurred fewer than 10 times. The occurrence and abundance models were fit using Bayesian methods, with the software JAGS 3.2.0 (Plummer 2012). Further details are in Appendix S1.

Model evaluation

Evaluation of model fits showed satisfactory agreement with distributional assumptions for the random effects and the residuals of the abundance model, and linearity of relationships with the continuous predictors. To evaluate the strength of support for our main hypotheses, we report 95% credible intervals for the interaction parameters γ_{nit*N}, $\gamma_{PAR*\mu 10}$ and $\gamma_{n*P*\mu max}$. We also report the per cent variation in slopes explained by the three functional traits. Additional visualisation of how the model fits interspecific variation in response to PAR, nitrate and nitrate*PAR is given in Figs S3–S5. Our hypotheses concern variation between species in the slope of response to environmental factors, and we focus on this variation in the Results; there is also considerable variation between species

Table 1 Parameter estimates for the occurrence and abundance models. For each parameter, the posterior mean and 95% credible interval, calculated as the highest posterior density (HPD) interval, is reported

	(a) Presence/absence model		(b) Abundance model	
	Mean	95% HPD int.	Mean	95% HPD int.
$\overline{b_0}$	−1.97	(−4.38, 0.22)	6.65	(2.88, 10.4)
$\overline{b_{nit}}$	−0.13	(−1.61, 1.21)	−0.39	(−2.09, −0.81)
$\overline{b_{PAR}}$	0.48	(−0.56, 1.74)	−0.70	(−1.72, −0.36)
$\overline{b_{n*P}}$	0.13	(−0.42, 0.60)	0.54	(0.28, 0.97)
$\gamma_{\mu 10}$	0.64	(−2.10, 3.03)	−1.05	(−4.75, 3.46)
γ_N	0.86	(−1.81, 3.45)	−1.39	(−4.19, 3.74)
$\gamma_{\mu max}$	0.69	(−1.87, 3.69)	0.62	(−4.61, 5.23)
$\gamma_{PAR*\mu 10}$	−1.29	(−2.24, −0.31)	−0.15	(−0.71, 0.34)
γ_{nit*N}	0.12	(−1.32, 1.71)	−0.55	(−1.07, −0.15)
$\gamma_{nit*\mu max}$	−0.68	(−2.41, 1.15)	−0.70	(−1.31, −0.06)
$\gamma_{PAR*\mu max}$	−1.80	(−3.06, −0.46)	−0.95	(−1.63, −0.31)
$\gamma_{N*P*\mu max}$	0.16	(−0.44, 0.85)	0.48	(0.15, 0.83)
σ_0	3.96	(1.54, 6.26)	4.46	(1.55, 9.31)
σ_{nit}	2.09	(0.68, 3.37)	0.38	(0.003, 0.95)
σ_{PAR}	1.18	(0.001, 2.20)	0.33	(0.0012, 0.96)
σ_{n*P}	0.36	(0.0002, 0.71)	0.18	(9.7e-5, 0.49)
ρ	1.77	(1.29, 2.27)	0.26	(0.12, 0.40)
σ_ν	NA		1.45	(1.35, 1.56)

in average probability of occurrence and average abundance, as well as residual variation not explained by species identity (Table 1). Explanation of this variation in future work will presumably require additional environmental factors and traits related to those factors, or a more mechanistic model of community dynamics.

RESULTS

The occurrence model shows that there is substantial interspecific variation in how light availability affects the probability of presence, with most species more likely to be present as PAR increases, but a few more likely to be present as PAR decreases (Figs 3a and S3). This variation can be partially explained by μ_{10} in support of our *a priori* prediction that species with more positive μ_{10} will have a less positive or more negative response to PAR (Figs 2b and 3a). The posterior mean of $\gamma_{PAR*\mu 10}$ is −1.29, with a 95% highest posterior density (HPD) credible interval of (−2.24, −0.31). The posterior mean of the partial R^2, quantifying the variation in slopes explained by μ_{10}, is 63% (95% HPD interval = (14%, 100%)). There is also interspecific variation in the effect of nitrate on presence, and perhaps in the effect of nitrate*PAR, but this variation is not explained by N_{saff} or $\mu_{\max}$ (Table 1).

The abundance model supports our predictions regarding the effects of N_{saff} and $\mu_{\max}$ on interspecific variation in response to nitrate and nitrate*PAR. All species tend to be more abundant when nitrate is low or when nitrate*PAR is high (Figs 3b,c and S4–S5). γ_{nit*N} has a posterior mean of −0.55 (95% HPD interval = (−1.07, −0.15)), indicating that species with greater N_{saff} increase more steeply as nitrate decreases (Table 1; Figs 2a and 3b), and the posterior mean of variation in slopes explained is 72% (95% HPD interval = (10, 100)). Likewise, $\gamma_{N*P*\mu max}$ has a posterior mean of 0.48 (95% HPD interval = (0.15, 0.83)), indicating that species with greater $\mu_{\max}$ increase more steeply as nitrate*PAR increases (Table 1; Figs 2c and 3c), and the posterior mean of variation in slopes explained is 82% (95% HPD interval = (34, 100)). In contrast, interspecific variation in the effect of light on abundance is not explained by μ_{10} (Table 1).

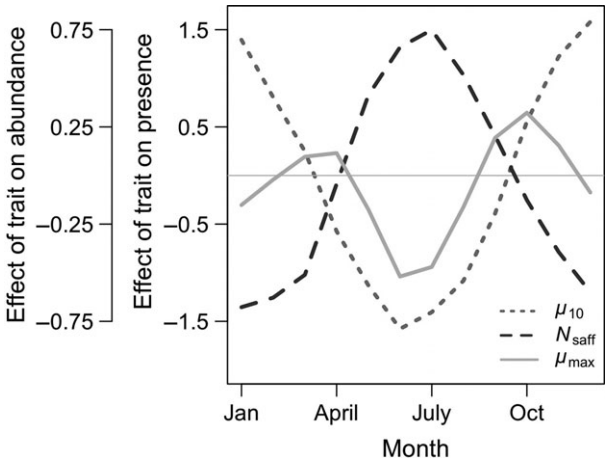

Figure 4 Seasonal variation in the relationship between traits and abundance. Model predictions are plotted for intra-annual variation in the relationship between functional traits and abundance/occurrence. Mean monthly conditions across years are used, to illustrate typical environmental variation and how this variation is predicted to alter the relationship between traits and abundance/occurrence. For μ_{10}, the scale is logit(p), where p is probability of presence. The line is obtained by multiplying mean monthly PAR by the posterior mean of $\gamma_{PAR*\mu 10}$. For N_{saff} and $\mu_{\max}$, the scale is log(V), where V is biovolume, and the lines are obtained by multiplying mean monthly nitrate by the posterior mean of γ_{nit*N}, and mean monthly nitrate*PAR by the posterior mean of $\gamma_{n*P*\mu max}$, respectively.

The trait-environment interactions we have tested can also be interpreted as quantifying temporal variation in the slope of abundance (or probability of occurrence) vs. trait values. For example, in the abundance model, γ_{nit*N} quantifies how the slope of log biovolume vs. N_{saff} changes as a function of nitrate availability, while accounting for variation in abundance caused by PAR and nitrate*PAR, and accounting for the fact that species differ in mean abundance across environmental conditions (quantified by the β_0^i's in eqn 3). In Fig. 4, we take advantage of this fact to plot how trait-abundance relationships are predicted to change over the course of a year, using mean monthly conditions across years. In essence, this plot shows typical intraannual environmental variation (Fig. 1), multiplied by the model parameters that quantify how the environmental factors alter trait-abundance relationships. Thus, the effect of μ_{10} on occurrence is most beneficial during the winter when PAR is low; the effect of N_{saff} on abundance is most beneficial during the summer when nitrate is low; and the effect of $\mu_{\max}$ on abundance is most beneficial during the spring and fall when both nitrate and PAR are relatively abundant.

DISCUSSION

Our analysis shows that lab-measured functional traits of phytoplankton are effective predictors of variation in how species respond to seasonal fluctuation in the Western English Channel. Species with a greater tolerance of low light decline less strongly or even increase, in terms of probability of occurrence, as PAR becomes low in the well-mixed water column during winter (Fig. 3a); species with a higher maximum growth rate increase more steeply, in terms of abundance, during the favourable conditions of the spring and fall blooms (Fig. 3c); and species with a higher scaled nitrate affinity increase more steeply, in terms of abundance, as nitrate becomes scarce in the shallow summer mixed layer (Fig. 3b). The approach we have used allows us to consider shifting community trait structure, despite having trait information only for a subset of the community, because interspecific differences in the slope of response to environmental conditions leads to shifting relative abundances in the community (Fig. 2). These interspecific differences translate into seasonal variation in the relationships between traits and occurrence/abundance (Fig. 4). It is notable that the trait related to light limitation (μ_{10}) is predictive of interspecific variation in occurrence, while the traits related to nitrate limitation and maximum growth rate (N_{saff} and $\mu_{\max}$) are predictive of interspecific variation in abundance. This may be due to the fact that during the winter, many species are near or below the irradiance level required to maintain a positive growth rate (Fig. 3a), and thus, tolerance of low light determines whether a species is present at a detectable abundance.

Our results complement a growing body of work on terrestrial plants, showing that the trait structure of primary producer communities shifts in regular ways across environmental conditions (e.g. Cornwell & Ackerly 2009; Swenson & Weiser 2010). To our knowledge, this is the first demonstration of such patterns for the microbial communities that dominate ecosystem processes in the ocean. The factors we have investigated, light and nitrate, are two of the

dominant factors controlling ocean productivity, and our results show that these factors cause shifts in community structure that can be predicted based on commonly measured traits. We think there is great potential for further success in applying this approach to microbes, in part because the measurable traits are strongly linked to population dynamic processes, which allowed us to make *a priori* predictions of how the relative advantage of different traits would shift across environmental conditions.

Our analysis suggests that most of the variation in community structure of phytoplankton may be predictable based on a moderate number of key environmental factors. Although the temporal and spatial dynamics of individual species may be complex and difficult to predict, using the lens of functional trait structure may allow significant progress towards a more predictive community ecology. Additional traits likely to be important for phytoplankton include utilisation of Si, P and Fe, thermal tolerance, and resistance to grazers and viruses. Here, we have investigated the effect of temporal environmental variation, and we expect that similar patterns occur over spatial (vertical and horizontal) gradients.

It is noteworthy that functional traits measured on laboratory cultures are effective predictors of community responses under natural conditions. There are numerous reasons why lab-measured traits may not be predictive under natural conditions. The many studies from which we have compiled trait data do not use identical experimental methods; laboratory culture conditions differ from the natural environment in ways that are often difficult to account for; the cultured strains for which trait data were available were not necessarily strains isolated near the Western English Channel; trait data for individual species were typically compiled from multiple studies by different researchers. Nevertheless, the patterns we have found indicate that the traits typically measured by phytoplankton ecologists are robust indicators of interspecific variation, and we encourage the measurement of a greater number of traits on a broader range of species.

The approach we have used here tests whether functional traits can predict how a community changes as environmental conditions change. An important complementary issue for future research is the maintenance of trait diversity. For example, is temporal variation in the relative supply of light and nitrate sufficient to maintain the trait diversity present in the Western English Channel, with the relative advantage of different trait combinations shifting across seasons? How do processes such as trophic interactions affect the distribution of traits related to resource use? Addressing these questions will require a combination of statistical and experimental approaches, and mechanistic modelling of trait distributions in realistic environmental settings.

ACKNOWLEDGEMENTS

Oceanographic data from station L4, part of the Western Channel Observatory (www.westernchannelobservatory.org.uk), are funded under the UK Natural Environmental Research Council's National Capability. Tim Smyth, Claire Widdicombe, Malcolm Woodward and James Fishwick collected the WCO data used in this study. Mridul Thomas kindly shared μ_{max} data. Research was supported by NSF grants to EL and CAK. CAK was in part supported by the Marie Curie Fellowship from the EU. This is Kellogg Biological Station contribution no. 1706.

AUTHOR CONTRIBUTIONS

EL, KFE and CAK conceived the study; KFE developed statistical tools, carried out analyses and wrote the manuscript; EL and CAK commented on the manuscript

REFERENCES

Anderson, D.M., Cembella, A.D. & Hallegraeff, G.M. (eds.) (1998). *The Physiological Ecology of Harmful Algal Blooms*. Springer-Verlag, Heidelberg.

Berquist, A.M., Carpenter, S.R. & Latino, J.C. (1985). Shifts in phytoplankton size structure and community composition during grazing by contrasting zooplankton assemblages. *Limnol. Oceanogr.*, 30, 1037–1045.

Bouman, H.A., Ulloa, O., Barlow, R., Li, W.K.W., Platt, T., Zwirglmaier, K. *et al.* (2011). Water-column stratification governs the community structure of subtropical marine picophytoplankton. *Environ. Microbiol. Rep.*, 3, 473–482.

Boyd, P.W., Strzepek, R., Fu, F. & Hutchins, D.A. (2010). Environmental control of open-ocean phytoplankton groups: now and in the future. *Limnol. Oceanogr.*, 55, 1353–1376.

Briand, L.E. & Guillard, R.R.L. (1981). The effects of continuous light and light intensity on the reproductive rates of twenty-two species of marine phytoplankton. *J. Exp. Mar. Biol. Ecol.*, 50, 119–132.

Clark, J.S. (2007). *Models for Ecological Data: An Introduction*. Princeton University Press, Princeton, NJ.

Cornwell, W.K. & Ackerly, D.D. (2009). Community assembly and shifts in plant trait distributions across an environmental gradient in coastal California. *Ecol. Monogr.*, 79, 109–126.

Cunningham, R.B. & Lindenmayer, D.B. (2005). Modeling count data of rare species: some statistical issues. *Ecology*, 86, 1135–1142.

Droop, M.R. (1973). Some thoughts on nutrient limitation in algae. *J. Phycol.*, 9, 264–272.

Edwards, K.F., Klausmeier, C.A. & Litchman, E. (2011). Evidence for a three-way trade-off between nitrogen and phosphorus competitive abilities and cell size in phytoplankton. *Ecology*, 92, 2085–2095.

Edwards, K.F., Thomas, M.K., Klausmeier, C.A. & Litchman, E. (2012). Allometric scaling and taxonomic variation in nutrient utilization traits and maximum growth rate of phytoplankton. *Limnol. Oceanogr.*, 57, 554–566.

Eilers, P.H.C. & Peeters, J.C.H. (1988). A model for the relationship between light intensity and the rate of photosynthesis in phytoplankton. *Ecol. Model.*, 42, 199–215.

Elliott, J.A., Irish, A.E. & Reynolds, C.S. (2010). Modeling phytoplankton dynamics in fresh waters: affirmation of the PROTECH approach to simulation. *Freshw. Rev.*, 3, 79–96.

Eppley, R.W., Rogers, J.N. & McCarthy, J.J. (1969). Half-saturation constants for uptake of nitrate and ammonium by marine phytoplankton. *Limnol. Oceanogr.*, 14, 912–920.

Falkowski, P.G., Barber, R.T. & Smetacek, V. (1998). Biogeochemical controls and feedbacks on ocean primary production. *Science*, 281, 200–206.

Falkowski, P.G., Katz, M.E., Knoll, A.H., Quigg, A., Raven, J.A., Schofield, O. *et al.* (2004). The evolution of modern eukaryotic phytoplankton. *Science*, 305, 354–360.

Gelman, A. & Hill, J. (2006). *Data Analysis using Regression and Multilevel/Hierarchical Models*. Cambridge University Press, New York.

Grover, J.P. (1991). Dynamics of competition among microalgae in variable environments: experimental tests of alternative models. *Oikos*, 62, 231–243.

Harris, R. (2010). The L4 time-series: the first 20 years. *J. Plankton Res.*, 32, 577–583.

Healey, F.P. (1980). Slope of the monod equation as an indicator of advantage in nutrient competition. *Microbial Ecol.*, 5, 281–286.

Huisman, J., Sharples, J., Stroom, J.M., Visser, P.M., Kardinaal, W.E.A., Verspagen, J.M.H. *et al.* (2004). Changes in turbulent mixing shift competition for light between phytoplankton species. *Ecology*, 85, 2960–2970.

Johnson, Z.I., Zinser, E.R., Coe, A., McNulty, N.P., Woodward, E.M.S. & Chisholm, S.W. (2006). Niche partitioning among *Prochlorococcus* ecotypes along ocean-scale environmental gradients. *Science*, 311, 1737–1740.

Kirk, J.T.O. (1994). *Light and Photosynthesis in Aquatic Ecosystems*, 2nd edn. Cambridge University Press, Cambridge.
Kruk, C., Peeters, E.T.H.M., Van Nes, E.H., Huszar, V.L.M., Costa, L.S. & Scheffer, M. (2011). Phytoplankton community composition can be predicted best in terms of morphological groups. *Limnol. Oceanogr.*, 56, 110–118.
Landry, M.R., Ondrusek, M.E., Tanner, S.J., Brown, S.L., Constantinou, J., Bidigare, R.R. *et al.* (2000). Biological response to iron fertilization in the eastern equatorial Pacific (IronEx II). I. Microplankton community abundances and biomass. *Mar. Ecol. Prog. Ser.*, 201, 27–42.
Lawton, J.H. (1999). Are there general laws in ecology? *Oikos*, 84, 177–192.
Litchman, E. & Klausmeier, C.A. (2008). Trait-based community ecology of phytoplankton. *Annu. Rev. Ecol. Evol. Syst.*, 39, 615–639.
Longhurst, A.L. (2007). *Ecological Geography of the Sea*, 2nd edn. Academic Press, San Diego.
Margalef, R. (1978). Life forms of phytoplankton as survival alternatives in an unstable environment. *Oceanol. Acta*, 1, 493–509.
McGill, B.J., Enquist, B.J., Weiher, E. & Westoby, M. (2006). Rebuilding community ecology from functional traits. *Trends Ecol. Evol.*, 21, 178–185.
Moore, L.R., Goericke, R. & Chisholm, S.W. (1995). Comparative physiology of *Synechococcus* and *Prochlorococcus*: influence of light and temperature on growth, pigments, fluorescence and absorptive properties. *Mar. Ecol. Prog. Ser.*, 116, 259–275.
Norberg, J. (2004). Biodiversity and ecosystem functioning: a complex adaptive systems approach. *Limnol. Oceanogr.*, 49, 1269–1277.
Passarge, J., Hol, S., Escher, M. & Huisman, J. (2006). Competition for nutrients and light: stable coexistence, alternative stable states, or competitive exclusion? *Ecol. Monogr.*, 76, 57–72.
Plummer, M. (2012). Just Another Gibbs Sampler (JAGS). Available at: http://mcmc-jags.sourceforge.net/. Last accessed 25 September 2012.
Rasband, W.S. (2011). *ImageJ*. U.S. National Institutes of Health, Bethesda, Maryland, USA, http://imagej.nih.gov/ij/
Schwaderer, A.S., Yoshiyama, K., Pinto, P.T., Swenson, N.G., Klausmeier, C.A. & Litchman, E. (2011). Eco-evolutionary differences in light utilization traits and distributions of freshwater phytoplankton. *Limnol. Oceanogr.*, 56, 589–598.
Smith, V.H. (1983). Low nitrogen to phosphorus ratios favor dominance by blue-green algae in lake phytoplankton. *Science*, 221(4611), 669–671.
Smyth, T.J., Fishwick, J.R., Al-Moosawi, L., Cummings, D.G., Harris, C., Kitidis, V. *et al.* (2010). A broad spatio-temporal view of the Western English Channel observatory. *J. Plankton Res.*, 32, 585–601.
Sterner, R. & Elser, J.J. (2002). *Ecological Stoichiometry*. Princeton University Press, Princeton.
Stomp, M., Huisman, J., Vörös, L., Pick, F.R., Laamanen, M., Haverkamp, T. *et al.* (2007). Colourful coexistence of red and green picocyanobacteria in lakes and seas. *Ecol. Lett.*, 19, 290–298.
Swenson, N.G. & Weiser, M.D. (2010). Plant geography upon the basis of functional traits: an example from eastern North American trees. *Ecology*, 91, 2234–2241.
Thomson, R.E. & Fine, I.V. (2003). Estimating mixed layer depth from oceanic profile data. *J. Atmos. Ocean. Tech.*, 20, 319–329.
Tilman, D. (1977). Resource competition between plankton algae: an experimental and theoretical approach. *Ecology*, 58, 338–348.
Tilman, D., Kilham, S.S. & Kilham, P. (1982). Phytoplankton community ecology: the role of limiting nutrients. *Ann. Rev. Ecol. Sys.*, 13, 349–372.
Webb, C.T., Hoeting, J.A., Ames, G.M., Pyne, M.I. & Poff, N.L. (2010). A structured and dynamic framework to advance traits-based theory and prediction in ecology. *Ecol. Lett.*, 13, 267–283.
Widdicombe, C.E., Eloire, D., Harbour, D., Harris, R.P. & Somerfield, P.J. (2010). Long-term phytoplankton community dynamics in the Western English Channel. *J. Plankton Res.*, 32, 643–655.

SUPPORTING INFORMATION

Additional Supporting Information may be downloaded via the online version of this article at Wiley Online Library (www.ecologyletters.com).

As a service to our authors and readers, this journal provides supporting information supplied by the authors. Such materials are peer-reviewed and may be re-organised for online delivery, but are not copy-edited or typeset. Technical support issues arising from supporting information (other than missing files) should be addressed to the authors.

Editor, James Elser
Manuscript received 30 July 2012
First decision made 31 August 2012
Manuscript accepted 6 September 2012